LSE_{20}-Mode Characteristics in Phase-Shifter Parametrization

G. N. TSANDOULAS, MEMBER, IEEE, FRANK G. WILLWERTH, MEMBER, IEEE, AND WILLIAM J. INCE

Abstract—The validity of considering the LSE_{20}-mode propagation threshold as the limiting factor in selecting rectangular-waveguide ferrite-phase-shifter dimensions is examined theoretically and experimentally using a dielectric model. Depending on the effective dielectric constant of the loading material, it is shown that the LSE_{20}-mode cutoff may, in many cases, be exceeded without introducing spurious mode resonances.

In addition, the effect of magnetization on the y-independent modal cutoffs is investigated. It is concluded that the dielectric model represents a worst case condition as far as higher order mode propagation is concerned.

Introduction

THE DESIGN of practical digital-latching-ferrite phase shifters in rectangular waveguide involves the selection of parameters and physical dimensions which will, as a rule, allow the excitation and propagation of some higher order modes. These, in turn, manifest themselves as sharp spikes[1] in the VSWR of the device. These spikes may be troublesome when the phase shifter is used as the beam-steering element in a phased-array radar. For example, they can ultimately cause the appearance of objectionable deep notches in the phased-array pattern. The problem becomes particularly serious in wide-band operation when multiple spikes may be generated for each propagating mode. Resistive film suppressors have been shown to be very effective [1] in suppressing the spikes due to the first two higher order LSE_{11} and LSM_{11} modes without impairing the overall match and without affecting the phase shift or appreciably degrading the power handling capability of the device.

The effectiveness of this suppressing mechanism depends on positioning the resistive film at a plane that contains a maximum-strength electric-field component of the undesired mode. At the same time the fundamental LSE_{10} wave is undisturbed, its electric vector being orthogonal to the plane of the suppressor. However, this is true for all LSE_{m0} (TE_{m0}) modes as well. For this reason the cutoff threshold for the LSE_{20} is regarded as imposing an upper limit in the selection of parameter values.

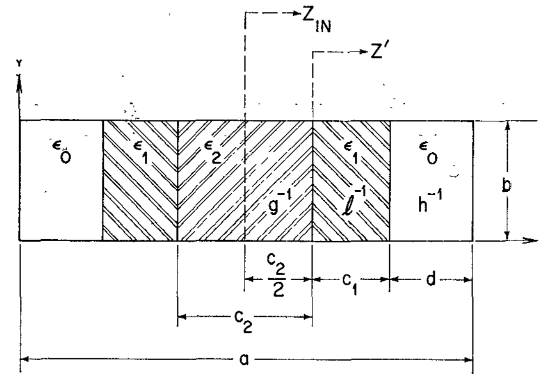

Fig. 1. The loaded waveguide geometry. g^{-1}, l^{-1}, and h^{-1} are transverse propagation constants.

Our aim in this paper is threefold. First, design guidelines are presented based on cutoff properties for the LSE_{20} mode in a pure dielectric model. Second, the very validity of the LSE_{20} limitation is examined experimentally in view of certain questions raised by us regarding the character of the mode. The reasoning is as follows: The LSE_{m0} part of the eigenmode spectrum of the differential operator appropriate to the problem shown in Fig. 1 is composed of modes whose field configuration is either symmetric, $LSE_{2m+1,0}$, or antisymmetric, $LSE_{2m,0}$, about the line $x=a/2$. Thus the symmetric structure of Fig. 1 should tend to excite the symmetric modes only, so that even if conditions are such that the LSE_{20} may propagate, it need not cause concern since it would not be excited to begin with. This means that the LSE_{30} emerges as the parameter limiting higher order mode.[2]

It has been shown [2] that phase-shifter low-power performance can be improved by dielectrically loading the toroid slot with a high dielectric constant material. For such devices, the even–odd mode argument becomes uncertain, since tolerances start playing an increasingly important role in that they may introduce enough asymmetry to launch the LSE_{20} mode. It was

Manuscript received March 31, 1971; revised June 1, 1971. This work was sponsored by the Department of the Army.
G. N. Tsandoulas and F. G. Willwerth are with the M.I.T. Lincoln Laboratory, Lexington, Mass. 02173.
W. J. Ince is with the M.I.T. Lincoln Laboratory, Lexington, Mass., and the Department of Electrical Engineering, Massachusetts Institute of Technology, Cambridge, Mass.

[1] In an actual device, the presence of such necessary components as the switching wire will launch a TEM wave which can also introduce VSWR spikes. This TEM mode will not be dealt with here.

[2] A practical example of symmetric-mode-only excitation is the "box" horn [3] which excites the TE_{10} and the TE_{30} but not the TE_{20}.

therefore decided to attempt to resolve the question experimentally, and the results are presented here.

A third objective involved the desire to gain some understanding of the effect of magnetization on the cutoffs of the LSE_{m0} modes so as to further corroborate the validity of the already established pure dielectric model [1].

Characteristic Equations—Dielectric Case

Fig. 2 shows two types of flux-driven nonreciprocal remanence-ferrite phase shifters in rectangular waveguide. Fig. 2(a) illustrates one type of device which employs a single-ferrite toroid completely contained within the guide [4], whereas the device of Fig. 2(b) is a composite circuit phaser with external flux path [5], [6].

For the determination of the resulting phase shifts, the twin-slab model of Fig. 1 is applicable [7]. This is dominant LSE_{10}-mode operation. For higher order propagation effects, the dielectric twin-slab is appropriate for Fig. 2(b), and is a reasonable approximation of Fig. 2(a). However, it has been established that the single-dielectric-slab model is sufficient [1] for computing cutoff frequencies, at least for the longitudinal section type of mode.

The characteristic equation for Fig. 1 may be obtained by a variety of methods. One may use the field-solution approach [1], [8] or the transfer matrix method utilized by Seidel [9] and subsequently by Gardiol [10]. A more direct method for our purposes is the open-and-short-circuit bisection transverse equivalent transmission line described by Collin [11]. Thus the transverse input impedance Z_{IN} is

$$Z_{IN} = \frac{1}{g} \frac{Z' + jg^{-1} \tan\left(\frac{gc_2}{2}\right)}{g^{-1} + jZ' \tan\left(\frac{gc_2}{2}\right)} \tag{1}$$

where

$$Z' = \frac{1}{l} \frac{jh^{-1} \tan(hd) + jl^{-1} \tan(lc_1)}{l^{-1} - h^{-1} \tan(hd) \tan(lc_1)} \tag{2}$$

and g^{-1}, l^{-1}, and h^{-1} are transverse propagation constants given by

$$g^2 = -\beta^2 - \left(\frac{n\pi}{b}\right)^2 + \epsilon_{r_2} k_0^2 \tag{3}$$

$$l^2 = -\beta^2 - \left(\frac{n\pi}{b}\right)^2 + \epsilon_{r_1} k_0^2 \tag{4}$$

$$h^2 = -\beta^2 - \left(\frac{n\pi}{b}\right)^2 + k_0^2 \tag{5}$$

for a propagation factor of the form $\exp(j\beta z)$.

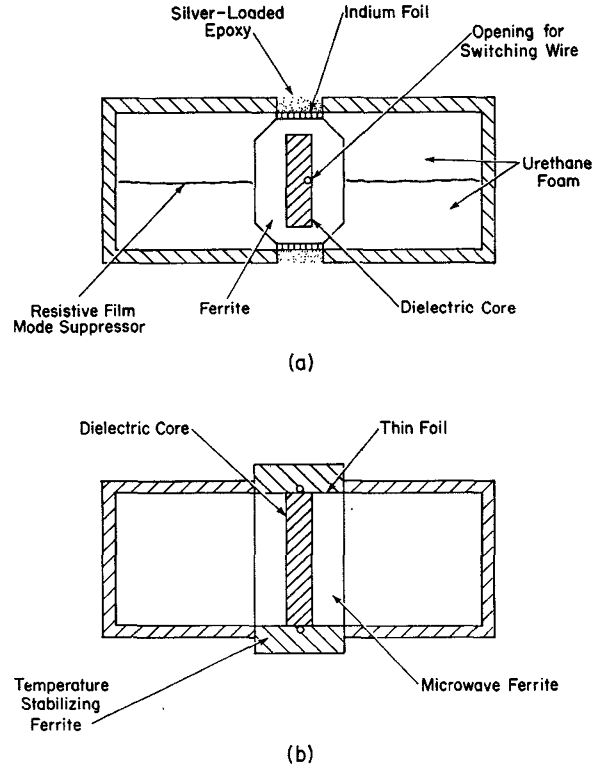

Fig. 2. (a) Cross section of single-toroid-ferrite phase shifter. (b) Cross section of composite-ferrite phase shifter.

The condition $Z_{IN} \rightarrow \infty$ yields the symmetric $LSE_{2m+1,n}$ modes, while the condition $Z_{IN} \rightarrow 0$ gives the antisymmetric $LSE_{2m,n}$ modes.

After some manipulation, the characteristic equations are for $LSE_{2m+1,n}$, or symmetric modes:

$$l[h \cot hd \cot lc_1 - l] \cot \frac{gc_2}{2} - g[l \cot lc_1 + h \cot hd] = 0. \tag{6}$$

For $LSE_{2m,n}$, or antisymmetric modes:

$$l[h \cot hd \cot lc_1 - l] + g[l \cot lc_1 + h \cot hd] \cot \frac{gc_2}{2} 0. \tag{7}$$

Cutoff contour plots based on these relationships are shown in Figs. 3 and 4. If the operating point falls below the appropriate curve, the mode in question is cutoff, while if it falls above the curve, the mode is propagating.

Fig. 3 corresponds to cases for which the single-slab model is adequate. It was used to compute slab dimensions for the experimental work described below. Fig. 4(a) and (b) are for the twin-slab configuration, and represent cutoff contours for the LSE_{20} mode only. The outer-slab dielectric constant ϵ_{r_1} has been taken as equal to 15 throughout this work, corresponding to typical garnet polycrystalline material.

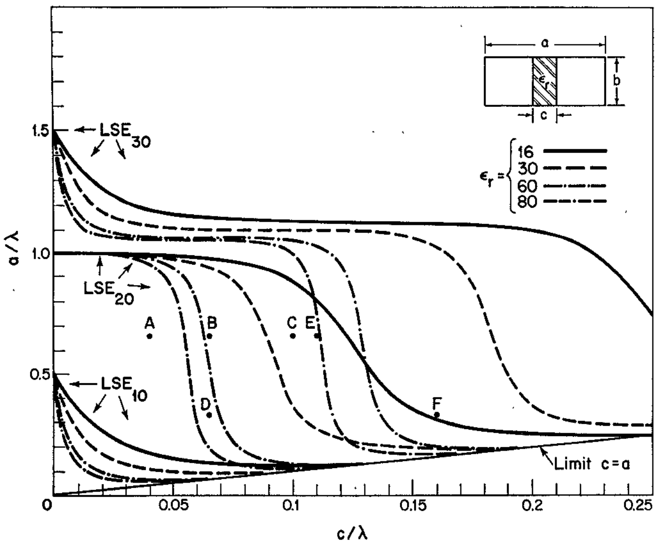

Fig. 3. Cutoff characteristics for the first three height-independent modes for a singly loaded waveguide. a/λ and c/λ are cutoff values of these parameters. Points A, B, C, D, E, and F are used in connection with Figs. 5 and 6.

These figures may be used as guidelines in selecting phaser dimensions in the frequency range of interest. (It is assumed that mode suppressors are used to suppress the first higher order LSE_{11} and LSM_{11} modes.) As such they provide an answer to the question of mode propagation. The second important question, that of excitation, is considered next.

Experimental Results

VSWR and transmission measurements were made using a singly loaded waveguide at C band. The slab length was 3 in. Fig. 5 shows some of the results for a material with $\epsilon_r = 60$. In Fig. 5 dimensions were chosen so that the LSE_{20} mode is the highest order mode to propagate. Good wide-band matching was obtained by properly designed dielectric transformers. It is seen that three main resonance peaks are produced. They were all identified as being due to LSE_{20}-mode resonances. This was done by calculating λ/λ_g curves for this mode from (7), and by showing that the frequency separations of the peaks is just wide enough to correspond to a path length of 360 electrical degrees for the 6-in round-trip length of the sample. To ensure the sole presence of the LSE_{20} mode, the LSE_{11} and LSM_{11} modes were driven into cutoff by choosing a sufficiently low waveguide height. The plot shows that the mode is definitely excited, in spite of the fact that a very symmetrical physical configuration was used.

Fig. 5(b)–(d) shows VSWR plots for various operating points near the $\epsilon_r = 60$ cutoff curve in Fig. 3. An amount of mismatching was introduced on purpose to show the details of the characteristic more clearly. No resonances of any kind were encountered, so it can be concluded that the mode requires rather favorable conditions in order to be excited.

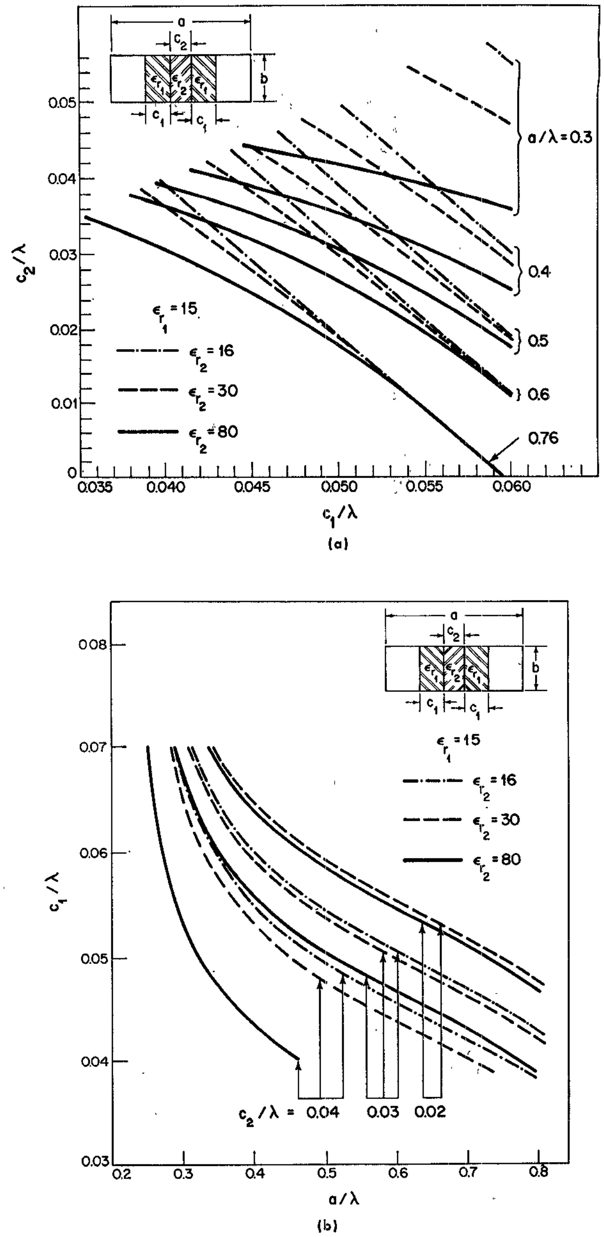

Fig. 4. LSE_{20}-mode cutoff contours for twin-slab loaded waveguides. Mode is cutoff if operating point falls below the appropriate curve. Mode is propagating if operating point falls above the appropriate curve.

To determine whether the high dielectric constant of the material was a major contributing factor in the excitation of the mode in Fig. 5(a), a second experiment was performed using $\epsilon_r = 30$. Fig. 6(a) is a plot for a point of operation near but above cutoff, yet no resonances were observed. In Fig. 6(b) conditions are such that the mode is well into the propagating region. Some LSE_{20} moding is observed over a very wide frequency band. Similar results, with slight moding, were obtained with a dielectric constant of 40.

These results show the importance played by the dielectric constant of the materials in LSE_{20}-mode excitation. A structure with an effective dielectric constant

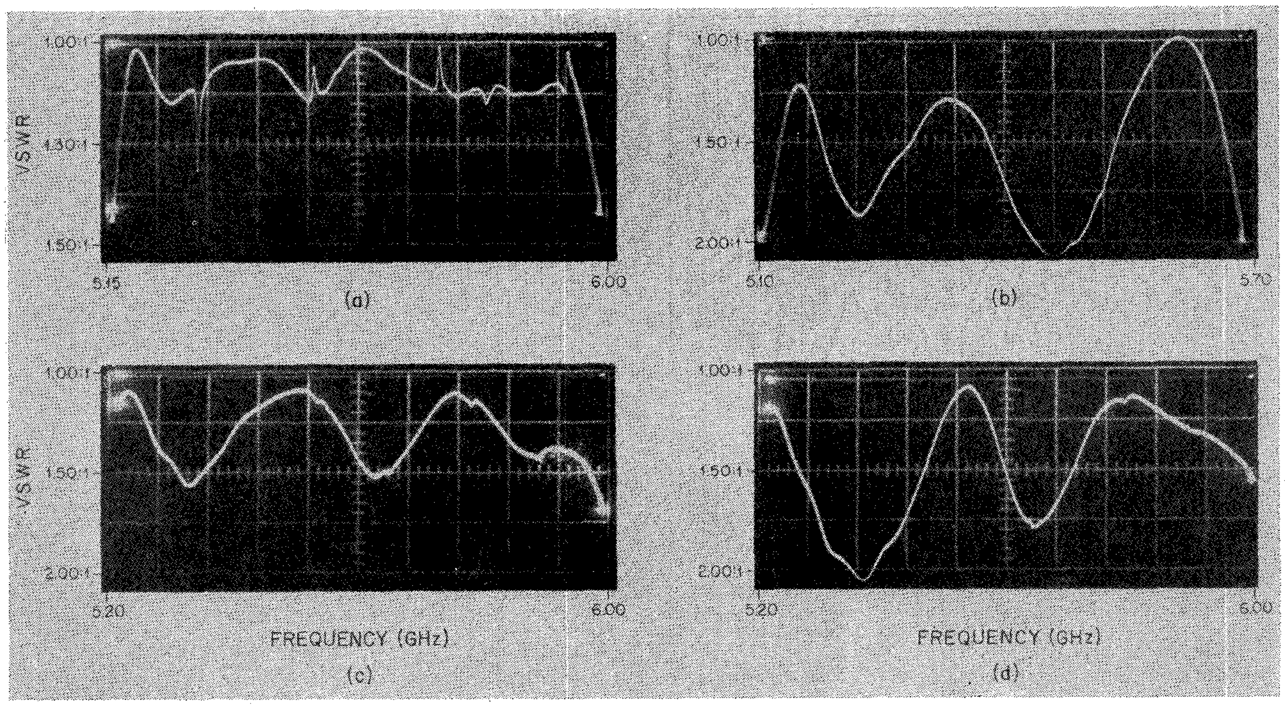

Fig. 5. Experimental VSWR results for singly loaded waveguide and for several combinations of dielectric and guide widths showing the onset of the LSE_{20} resonance. In all cases $b/\lambda_0=0.06$, $\epsilon_r=60$. Design center frequency $f_0=5.7$ GHz. (a) $c/\lambda_0=0.1$, $a/\lambda_0=0.66$ (point C in Fig. 3). (b) $c/\lambda_0=0.04$, $a/\lambda_0=0.66$ (point A in Fig. 3). (c) $c/\lambda_0=0.065$, $a/\lambda_0=0.66$ (point B in Fig. 3). (d) $c/\lambda_0=0.065$, $a/\lambda_0=0.33$ (point D in Fig. 3).

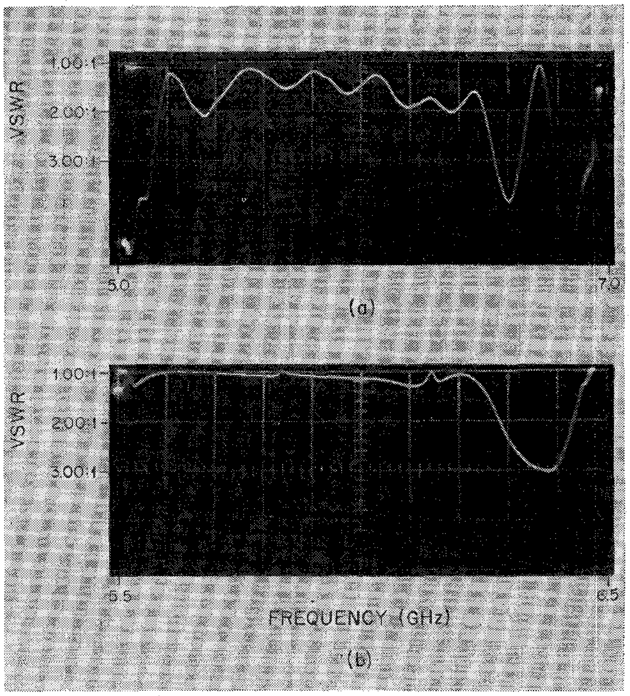

Fig. 6. VSWR versus frequency for a slab with $\epsilon_r=30$. Design center frequency is 5.7 GHz, $b/\lambda_0=0.06$. (a) $c/\lambda_0=0.11$, $a/\lambda_0=0.66$ (point E in Fig. 3). (b) $c/\lambda_0=0.16$, $a/\lambda_0=0.33$ (point F in Fig. 3).

of about 40 or higher requires a filling factor not too far above the theoretically predicted one for launching the LSE_{20} mode. As the dielectric constant decreases, the equivalent filling factors must be increased substantially beyond those implied by Figs. 3 and 4 for the mode to be excited.

The Effect of Magnetization

As has been mentioned above, the dielectric model has been shown to be a good approximation of the phaser structure when mode-propagation questions arise. For the general modes it is the only exactly solvable model when magnetization is applied. Cutoff relations for the $LSE_{m,0}$-type modes may, however, be obtained using the same method employed in the dielectric case. In our case, with magnetization transverse to the direction of propagation, the permeability $\overleftrightarrow{\mu}$ takes the form

$$\overleftrightarrow{\mu} = \mu_0 \begin{bmatrix} \mu' & 0 & -j\kappa \\ 0 & 1 & 0 \\ j\kappa & 0 & \mu' \end{bmatrix} \quad (8)$$

$$\kappa = -\frac{\gamma\mu_0 M_r}{\omega} \quad (9)$$

where γ is the gyromagnetic ratio and M_r is the remanent magnetization. It is assumed that the internal magnetic field is zero in the remanent state.

The cutoff relations follow from the transverse input impedance expression (1) with the introduction of an effective permeability in the appropriate transverse propagation factor. Thus

$LSE_{2m+1,0}$ modes

$$[\sqrt{\mu' g}\cot H \cot F - \sqrt{\epsilon_{r_1}}]\cot G - \sqrt{\frac{\epsilon_{r_2}}{\epsilon_{r_1}}}\,\mu' g\,[\sqrt{\epsilon_{r_1}}\cot F + \sqrt{\mu' g}\cot H] = 0. \quad (10)$$

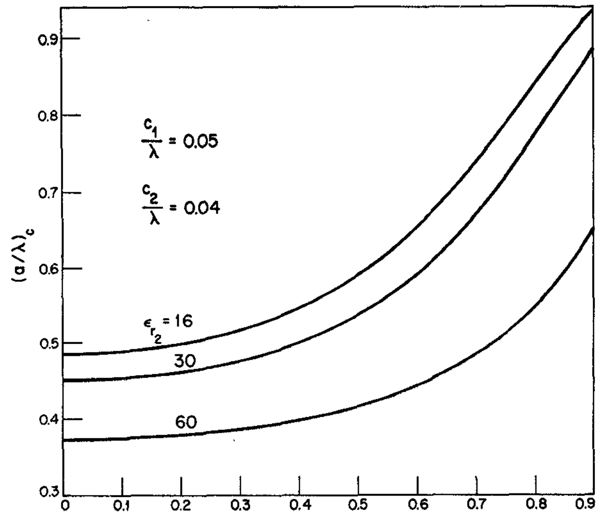

Fig. 7. LSE_{20}-mode dependence of cutoff value of a/λ on magnetization. $[\kappa = (-\gamma\mu_0 M_r)/(\omega)]$. Cutoff value is raised as κ increases. $\epsilon_{r_1} = 15$.

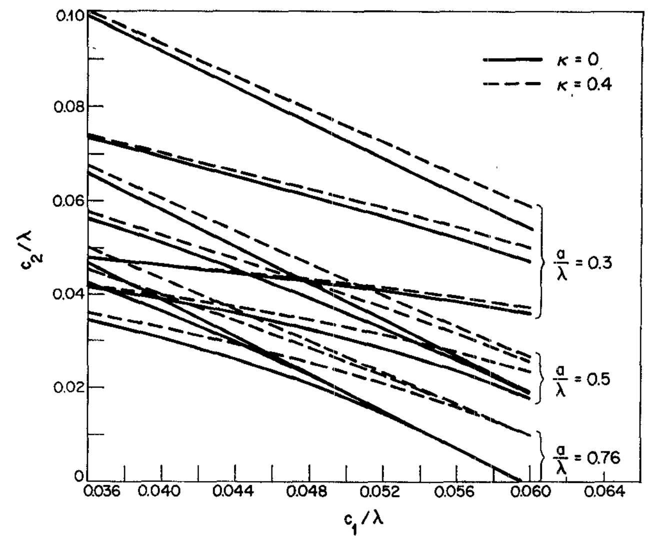

Fig. 8. LSE_{20}-mode cutoff contours for two values of κ. Within each family there are three curves corresponding to $\epsilon_{r_2} = 16$, 30, and 60 from top to bottom.

$LSE_{2m,0}$ modes

$$\sqrt{\mu' g} \cot H \cot F - \sqrt{\epsilon_{r_1}} + \sqrt{\frac{\epsilon_{r_2}}{\epsilon_{r_1}} \mu' g} \left[\sqrt{\epsilon_{r_1}} \cot F + \sqrt{\mu' g} \cot H\right] \cot G = 0 \quad (11)$$

where

$$F = 2\pi\sqrt{\epsilon_{r_1}\mu' g}\left(\frac{c_1}{\lambda}\right) \quad (12)$$

$$G = \pi\sqrt{\epsilon_{r_2}}\left(\frac{c_2}{\lambda}\right) \quad (13)$$

$$H = \pi\left(\frac{a}{\lambda} - \frac{c_2}{\lambda} - \frac{2c_1}{\lambda}\right) \quad (14)$$

$$g = 1 - \left(\frac{\kappa}{\mu'}\right)^2, \qquad \mu' g = \mu_{\text{eff}}. \quad (15)$$

Equation (10) is the same as that obtained from an earlier work [7] under the restriction $\lambda/\lambda_g = 0$. It is seen that the cutoff expressions are independent of the sign of the magnetization M_r.

A plot of the cutoff value of a/λ for the LSE_{20} mode versus κ is shown in Fig. 7. The important feature of these curves is that they have a positive slope. This implies that the effect of magnetization is to raise the cutoff point so that the dielectric model actually represents worst case conditions. Similar behavior is exhibited in Fig. 8 in which cutoff conditions at the representative, if slightly high, value $\kappa = 0.4$ are compared with those for the dielectric model. (For remanent devices the range $0.2 \leq |\kappa| \leq 0.4$ is typical.)

In the above expressions the value of μ' was taken as equal to unity, which is a realistic condition under the assumption of zero internal magnetizing field. Departures from this value, as for instance in the case of partially magnetized ferrites [12], will not materially affect the results.

Conclusions

In this paper we have examined the propagation characteristics of the LSE_{20} mode in dielectrically loaded rectangular waveguides. Using theoretical guidelines, experimental evidence was obtained pointing to the important role this mode may play in the selection of phase-shifter parameters. We conclude that for effective dielectric-constant loading, such that $\epsilon_r < 40$, one may safely exceed the propagation threshold for the LSE_{20} mode essentially without exciting it should other design factors make this necessary. With $\epsilon_r > 40$ one should generally not operate much beyond the LSE_{20} cutoff frequency.

It is also shown that the dielectric model is a worst case condition as far as LSE_{20}-mode propagation is concerned. A design based on parameter selection according to the dielectric model results in more favorable LSE_{20}-mode propagation conditions than a design in which magnetization is included. For this reason, the dielectric model should be of greater value in ensuring LSE_{20} nonexcitation. In an actual device, the presence of such necessary components as the switching wire will introduce some asymmetry. This may or may not have a decisive effect on LSE_{20} excitation. However, based on our previous experience with this phenomenon, it is believed that the switching wire will introduce a TEM component, but that the higher order modes will be largely unaffected.

References

[1] G. N. Tsandoulas, D. H. Temme, and F. G. Willwerth, "Longitudinal section mode analysis of dielectrically loaded rectangular waveguides with application to phase shifter design," *IEEE Trans. Microwave Theory Tech.*, vol. MTT-18, pp. 88–95, Feb. 1970.
[2] W. J. Ince, D. H. Temme, F. G. Willwerth, and R. L. Huntt, "The use of manganese-doped iron garnets and high dielectric constant loading for microwave latching ferrite phasers," in *IEEE G-MTT Int. Microwave Symp. Dig.*, pp. 327–329, May 1970.
[3] S. Silver, *Microwave Antenna Theory and Design* (M.I.T. Radia-

tion Laboratory Series), vol. 12. New York: McGraw-Hill, 1949.
[4] D. H. Temme, R. L. Huntt, R. G. West, and A. C. Blankenship, "A low-cost latching ferrite phaser fabrication technique," in *IEEE G-MTT Int. Microwave Symp. Dig.*, pp. 88–96, May 1969.
[5] E. Stern and A. Christopher, Microwave Chemicals Lab., M.I.T. Lincoln Lab., Subcontract 291, Final Rep., May 1964.
[6] E. Stern and W. J. Ince, "Temperature stabilization of unsaturated microwave ferrite devices," *J. Appl. Phys.*, vol. 37, pp. 1075–1076, 1966.
[7] W. J. Ince and E. Stern, "Nonreciprocal remanence phase shifters in rectangular waveguide," *IEEE Trans. Microwave Theory Tech.*, vol. MTT-15, pp. 87–95, Feb. 1967.
[8] P. H. Vartanian, W. P. Ayres, and A. L. Helgesson, "Propagation in dielectric slab loaded rectangular waveguide," *IRE Trans. Microwave Theory Tech.*, vol. MTT-6, pp. 215–222, Apr. 1958.
[9] H. Seidel, "Ferrite slabs in transverse electric mode waveguide," *J. Appl. Phys.*, vol. 28, pp. 218–226, 1957.
[10] F. E. Gardiol, "Higher-order modes in dielectrically loaded rectangular waveguides," *IEEE Trans. Microwave Theory Tech.*, vol. MTT-16, pp. 919–924, Nov. 1958.
[11] R. E. Collin, *Field Theory of Guided Waves*. New York: McGraw-Hill, 1951.
[12] E. Schlömann, "Microwave behavior of partially magnetized ferrites," *J. Appl. Phys.*, vol. 41, pp. 204–214, 1970.

Narrow-Bandpass Waveguide Filters

ALI E. ATIA, MEMBER, IEEE, AND ALBERT E. WILLIAMS, MEMBER, IEEE

Abstract—**A procedure is described whereby narrow-bandpass waveguide filters having ripple in both the passbands and stopbands can be synthesized in the form of coupled waveguide cavities. Orthogonal modes in square or circular waveguides are employed to enable negative coupling elements to be realized. As a consequence, very compact filters can be constructed. Experimental results on an 8-cavity orthogonal-mode narrow-bandpass filter are shown to agree well with theory.**

I. Introduction

IT HAS BEEN well known since the early work on filter synthesis by Darlington [1] and Cauer [2] that when frequency selectivity and bandpass loss are considered to be the important filtering properties, then the optimum filters are those exhibiting ripple in both passbands and stopbands.

However, the present design of narrow-bandpass waveguide cavity filters is largely based upon the work of Cohn [3], which realizes filters in the form of cascaded, synchronously tuned cavities exhibiting only monotonically increasing out-of-band attenuation. This restriction in filter design is principally due to the difficulty in transforming the optimum low-pass ladder networks to coupled-cavity structures.

Manuscript received April 5, 1971; revised July 16, 1971. This paper is based upon work performed in COMSAT Laboratories under Corporate sponsorship.
The authors are with COMSAT Laboratories, Clarksburg, Md. 20734.

Kurzrok [4] describes how extra coupling applied between the first and last cavity of a direct-coupled 4-coaxial-cavity structure produces a zero of transmission in the stopband. Easter and Powell [5] describe similar filters in rectangular waveguide. Recently, Williams [6] has illustrated the realization of the fourth-order elliptic function in an orthogonal-mode circular-waveguide structure.

It is the purpose of this paper to extend this work by describing the waveguide synthesis of general filter functions having these optimum-amplitude filtering properties. Two structures which employ orthogonal-mode waveguide cavities are presented, and extensive use is made of the general coupling-cavity theory that is outlined by Atia and Williams [7]. An experimental 8-cavity circular-waveguide bandpass filter with eight poles and two zeros of transmission is shown to correlate well with theory.

II. Theory

An account of the equivalent circuit of generally coupled cavities was given by Reiter [8], who described how Maxwell's equations can be replaced by an equivalent infinite system of algebraic inhomogeneous equations. However, if the frequency band of interest is narrow, so that each cavity can be treated as a single resonant circuit [9] with multiple couplings to other